Interband tunneling in a superlattice absorber

Andrzej Kolek
Department of Electronics Fundamentals, Rzeszów University of Technology, Rzeszów, Poland
e-mail: akoleknd@prz.edu.pl

INTRODUCTION

Superlattice (SL) photodiodes are now widely used to detect radiation, especially in the infrared region. However, in many cases their theoretical description merely adopt 'homogeneous' models [1]. In particular, the band-to-band (btb) tunneling is usually described with the Kane formula which was derived for a homojunction device [2]. This is because the vertical transport under high electric fields is almost unexplored for SL devices. In this paper the nonequilibrium Greens function (NEGF) method is used to study btb tunneling in SL absorber, with the aim of verifying the justification for the approaches that use 'homogeneous' models.

MODEL & METHOD

As the aim of the work is of qualitative rather than quantitative nature, the device is modelled with the two-band Hamiltonian

$$H = \begin{bmatrix} E_c(z,k) & \hbar\sqrt{\frac{E_p}{2m_0}}\frac{d}{dz} \\ \hbar\sqrt{\frac{E_p}{2m_0}}\frac{d}{dz} & E_\upsilon(z,k) \end{bmatrix}, \quad (1)$$

where z is the growth direction, k is the in-plane momentum norm, and $E_i(z, k) = E_i(z) \pm \hbar^2k^2/2m_{\|i}$, $i = c, \upsilon$, are k-dependent band edges. Calculations are made for a toy p-i-n diode made of 9 SL periods terminated with bulk n-InAs and p-GaSb leads. The leads, and adjacent to them parts of the SL region are doped to $n = p = 1\times10^{18}$ cm^{-3}. The band diagram of the device is shown in Fig. 1.

In the NEGF formalism the scatterings due to optical and acoustic phonons, and rough interfaces were included. The equations of the formalism, completed by the Poisson equation, were solved self-consistently (Born approximation).

RESULTS & CONCLUSIONS

Results of the simulations are shown in Figs. 1-4. Fig.1 illustrates, that at sufficiently high electric field F, the minibands break into the ladder of localized Wannier-Stark (WS) states [3]. They act as resonant centers for the btb tunneling process; each time the WS state in the conduction band (CB) aligns energetically with the WS state in the valence band (VB), the btb current is enhanced. The resulting, oscillatory structure of current-field characteristic is shown in Fig. 2. Similar effects were observed in real devices made of high-quality materials, in which defect-assisted tunneling did not hide the direct btb tunneling current, e.g. in ref. [4]. This means that the formulas derived for btb tunneling in a bulk material can hardly be used for SL materials. Further analyses performed on the simulation data, and illustrated in Fig. 3 and Fig. 4 allow to propose a new analytic formula for btb tunneling current in SL materials [5]. Namely,

$$J_{BTB} = N\frac{em_{\|,h}\delta E}{\pi\hbar^2 t_{tun}(m_F, \Delta E_F)}, \quad (2)$$

where N is the number of btb transitions (≅ SL periods), δE is the energetic width of tunneling current, t_{tun} is the (field-dependent) tunneling time of the dominant btb transition which spans m_F SL periods, and ΔE_F is the mismatch of WS energies.

ACKNOWLEDGMENT

This research was supported by the National Science Centre, Poland, project No. UMO-2020/35 /B/ST7/01830 (OPUS-19).

REFERENCES

[1] Delmas, M., Rodriguez, J. B., Rossignol, R., Licht, A. S., Giard, E., Ribet-Mohamed, I. & Christol, P. *Identification of limiting mechanism in GaSb-rich superlattice midwave infrared detector*. J. Appl. Phys. **119**, 174503 (2016).
[2] Pan, A., Chui, C., *Modeling direct interband tunneling. I. Bulk semiconductors*, J. Appl. Phys. **116**, 054508 (2014).
[3] Wacker, A. *Semiconductor superlattices: a model system for nonlinear transport*. Physics Reports **357**, 1 (2002).
[4] Kazemi, A., Myers, S., Taghipour, Z., Mathews, S., Schuler-Sandy, T., Lee, S. & Krishna, S. *Mid-wavelength infrared unipolar nBp superlattice photodetector*. Infrared Physics & Technology **88**, 114 (2018).
[5] Kolek, A. *Interband Tunneling in a Type-II Broken-gap Superlattice*, Phys. Rev. Applied **19,** 024059 (2023).

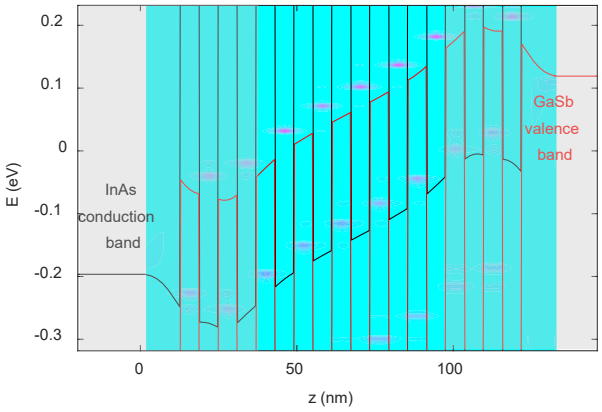

Fig. **1**. Band diagram of the p-i-n SL device with 6 nm InAs/6 nm GaSb period. Doped regions are shadowed. The undoped central part resembles the absorber in a real photodiode. The color map shows local density of states for the vanishing in-plane momentum, $k = 0$, calculated with the NEGF method.

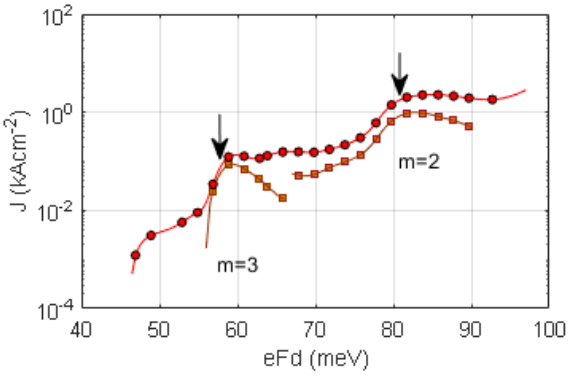

Fig. 2. Current-filed (I-V) characteristic (calculated). Arrows indicate the positions of the resonances, determined by the equation: $eF(m + 1/2)d = \Delta E_{SL}$ (d is the SL period, ΔE_{SL} is the C1-H1 bandgap and $m + 1/2$ is the number of SL periods spanned by the tunneling process) for $m = 2$ and $m = 3$. Series correspond to: circles - total current, squares/crosses - individual btb transitions between Wannier-Stark states.

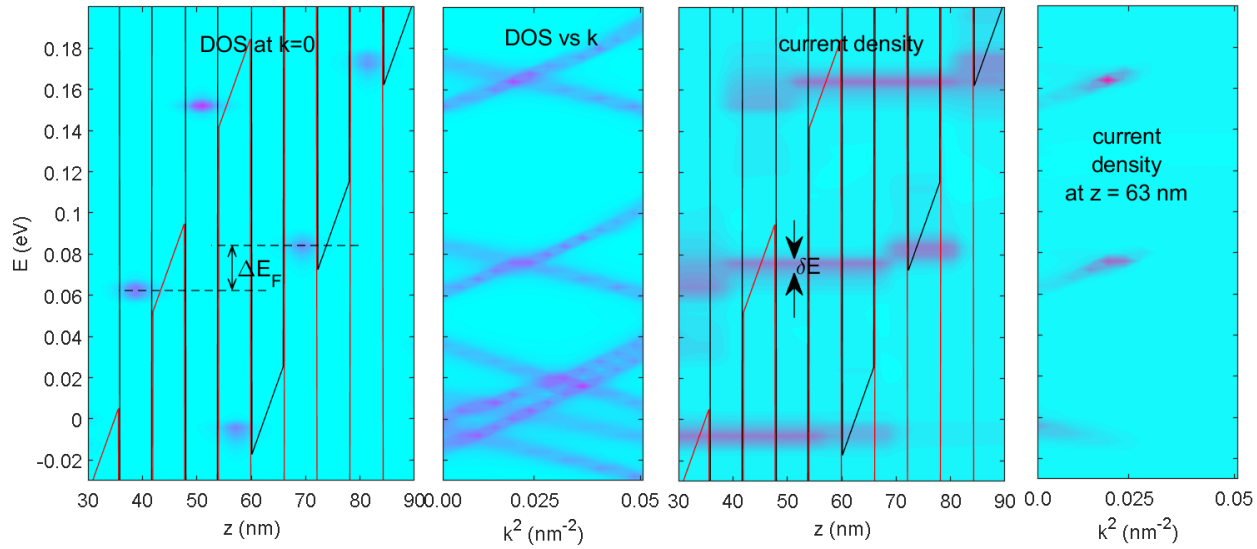

Fig. 3. (a) Band diagram and DOS for vanishing in-plane momentum $k = 0$ in the central part of the absorber under high electric field. Minibands are broken into WS states. ΔE_F is the (field dependent) mismatch between WS states involved in the interband tunneling transition (b) DOS as function of in plane momentum k; lines show hole and electron subbands formed by the WS states in C1 and H1 minibands. (c) Position resolved energetic spectrum of the current density; δE is energy width of the current strip (d) Momentum-energy resolved current density at $z = 63$ nm; current flows at k's for which electron and hole WS subbands cross.

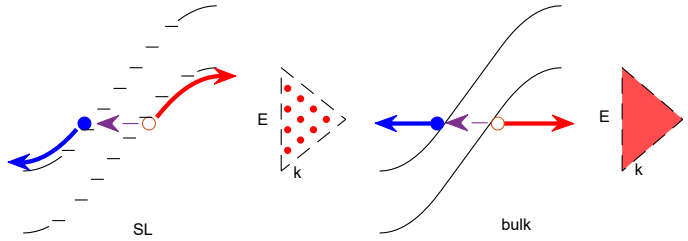

Fig. 4. Diagrams illustrating fundamental differences in btb tunneling current in bulk and SL devices in real and energy-momentum space: (i) the continuous vs discrete grid of energy-momentum pairs available for btb tunneling transitions (ii) ballistic vs inelastic extraction of created e-h pairs, which in SL is the LO-phonon dominated WS hopping within minibands [3].